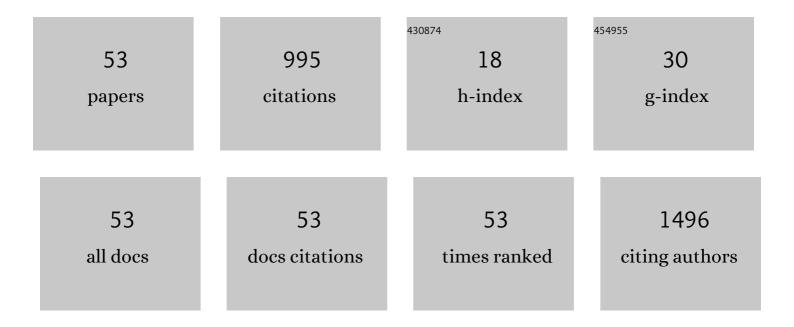
## Yan Huang

List of Publications by Year in descending order

Source: https://exaly.com/author-pdf/601850/publications.pdf Version: 2024-02-01



Υλη Ημανς

#	Article	IF	CITATIONS
1	Transcriptomic analysis of gills in nitrite-tolerant and -sensitive families of Litopenaeus vannamei. Comparative Biochemistry and Physiology Part - C: Toxicology and Pharmacology, 2022, 253, 109212.	2.6	2
2	Expressive Arts Therapy Combined with Progressive Muscle Relaxation following Music for Perioperative Patients with Gynecological Malignancies: A Pilot Study. Evidence-based Complementary and Alternative Medicine, 2022, 2022, 1-9.	1.2	1
3	Identification of a Novel Antimicrobial Peptide From the Ancient Marine Arthropod Chinese Horseshoe Crab, Tachypleus tridentatus. Frontiers in Immunology, 2022, 13, 794779.	4.8	2
4	Epigenomic profiling indicates a role for DNA methylation in the postnatal liver and pancreas development of giant pandas. Genomics, 2022, 114, 110342.	2.9	2
5	miR-731 modulates the zebrafish heart morphogenesis via targeting Calcineurin/Nfatc3a pathway. Biochimica Et Biophysica Acta - General Subjects, 2022, 1866, 130133.	2.4	0
6	ls chorioamnionitis associated with hearing impairment in preterm infants? A systematic review and meta-analysis. International Journal of Pediatric Otorhinolaryngology, 2022, 157, 111146.	1.0	1
7	Improving Satellite Waveform Altimetry Measurements With a Probabilistic Relaxation Algorithm. IEEE Transactions on Geoscience and Remote Sensing, 2021, 59, 4733-4748.	6.3	3
8	The interaction of ASIC1a and ERS mediates nerve cell apoptosis induced by insulin deficiency. European Journal of Pharmacology, 2021, 893, 173816.	3.5	5
9	Maternal Risk Factors for Lactation Mastitis: A Meta-analysis. Western Journal of Nursing Research, 2021, 43, 698-708.	1.4	13
10	Postoperative health-related quality of life of patients with gynecological malignancy: a meta-analysis. Supportive Care in Cancer, 2021, 29, 4209-4221.	2.2	3
11	Inonotsuoxide B regulates M1 to M2 macrophage polarization through sirtuin-1/endoplasmic reticulum stress axis. International Immunopharmacology, 2021, 96, 107603.	3.8	11
12	Caveolin-1 attenuates acetaminophen aggravated lipid accumulation in alcoholic fatty liver by activating mitophagy via the Pink-1/Parkin pathway. European Journal of Pharmacology, 2021, 908, 174324.	3.5	11
13	The lumbar region localization using bone anatomy feature graphs. Medical and Biological Engineering and Computing, 2021, 59, 2419-2432.	2.8	0
14	Acquirement of HRP conjunct IgG anti-IgMs from most widely cultured freshwater fishes in China and its immunoreactivity. Anais Da Academia Brasileira De Ciencias, 2021, 93, e20191024.	0.8	0
15	Current practices of peripheral intravenous catheter fixation in pediatric patients and factors influencing pediatric nurses' knowledge, attitude and practice concerning peripheral intravenous catheter fixation: a cross-sectional study. BMC Nursing, 2021, 20, 236.	2.5	3
16	Entropy Stabilization Effect and Oxygen Vacancies Enabling Spinel Oxide Highly Reversible Lithium-Ion Storage. ACS Applied Materials & Interfaces, 2021, 13, 58674-58681.	8.0	42
17	Zebrafish miR-462-731 is required for digestive organ development. Comparative Biochemistry and Physiology Part D: Genomics and Proteomics, 2020, 34, 100679.	1.0	6
18	Caveolin-1 alleviates lipid accumulation in NAFLD associated with promoting autophagy by inhibiting the Akt/mTOR pathway. European Journal of Pharmacology, 2020, 871, 172910.	3.5	31

Yan Huang

#	Article	IF	CITATIONS
19	Communicable disease mortality trends and characteristics of infants in rural China, 1996–2015. BMC Public Health, 2020, 20, 455.	2.9	6
20	In vivo and in vitro studies using Clonorchis sinensis adult-derived total protein (CsTP) on cellular function and inflammatory effect in mouse and cell model. Parasitology Research, 2020, 119, 1641-1652.	1.6	4
21	Alcohol promotes renal fibrosis by activating Nox2/4-mediated DNA methylation of Smad7. Clinical Science, 2020, 134, 103-122.	4.3	23
22	Self-assembly of nanoparticles by human serum albumin and photosensitizer for targeted near-infrared emission fluorescence imaging and effective phototherapy of cancer. Journal of Materials Chemistry B, 2019, 7, 1149-1159.	5.8	40
23	Imaging of anti-inflammatory effects of HNO <i>via</i> a near-infrared fluorescent probe in cells and in rat gouty arthritis model. Journal of Materials Chemistry B, 2019, 7, 305-313.	5.8	36
24	Detection of hypochlorous acid fluctuation <i>via</i> a selective near-infrared fluorescent probe in living cells and <i>in vivo</i> under hypoxic stress. Journal of Materials Chemistry B, 2019, 7, 2557-2564.	5.8	27
25	Rice Husk Ligninâ€Derived Porous Carbon Anode Material for Lithiumâ€lon Batteries. ChemistrySelect, 2019, 4, 4178-4184.	1.5	14
26	ls chorioamnionitis associated with neurodevelopmental outcomes in preterm infants? A systematic review and meta-analysis following PRISMA. Medicine (United States), 2019, 98, e18229.	1.0	15
27	A carbon dot-based fluorescent nanoprobe for the associated detection of iron ions and the determination of the fluctuation of ascorbic acid induced by hypoxia in cells and <i>in vivo</i> . Analyst, The, 2019, 144, 6609-6616.	3.5	28
28	Zebrafish miR-462-731 regulates hematopoietic specification and pu.1-dependent primitive myelopoiesis. Cell Death and Differentiation, 2019, 26, 1531-1544.	11.2	16
29	Central dicyanomethylene-substituted unsymmetrical squaraines and their application in organic solar cells. Journal of Materials Chemistry A, 2018, 6, 5797-5806.	10.3	25
30	Super-resolution imaging and real-time tracking lysosome in living cells by a fluorescent probe. Science China Chemistry, 2018, 61, 483-489.	8.2	18
31	Photovoltaic Devices Prepared through a Trihydroxy Substitution Strategy on an Unsymmetrical Squaraine Dye. Chemistry - A European Journal, 2018, 24, 3234-3240.	3.3	18
32	Clonorchis sinensis adult-derived proteins elicit Th2 immune responses by regulating dendritic cells via mannose receptor. PLoS Neglected Tropical Diseases, 2018, 12, e0006251.	3.0	14
33	Transcriptome comparison reveals insights into muscle response to hypoxia in blunt snout bream () Tj ETQq1 1	0.784314	rgBT/Overloc
34	The zebrafish miR-125c is induced under hypoxic stress via hypoxia-inducible factor 1α and functions in cellular adaptations and embryogenesis. Oncotarget, 2017, 8, 73846-73859.	1.8	10
35	Exploiting human walking speed transitions using a dynamic bipedal walking robot with controllable stiffness and limb coordination. , 2016, , .		1
36	The immunological characteristics and probiotic function of recombinant Bacillus subtilis spore expressing Clonorchis sinensis cysteine protease. Parasites and Vectors, 2016, 9, 648.	2.5	20

Yan Huang

#	Article	IF	CITATIONS
37	Interleukin-13 is involved in the formation of liver fibrosis in Clonorchis sinensis-infected mice. Parasitology Research, 2016, 115, 2653-2660.	1.6	18
38	Adding adaptable toe stiffness affects energetic efficiency and dynamic behaviors of bipedal walking. Journal of Theoretical Biology, 2016, 388, 108-118.	1.7	10
39	Investigation on oxidative stress of nitric oxide synthase interacting protein from Clonorchis sinensis. Parasitology Research, 2016, 115, 77-83.	1.6	7
40	Estimating Roof Solar Energy Potential in the Downtown Area Using a GPU-Accelerated Solar Radiation Model and Airborne LiDAR Data. Remote Sensing, 2015, 7, 17212-17233.	4.0	48
41	CsRNASET2 is an important component of Clonorchis sinensis responsible for eliciting Th2 immune response. Parasitology Research, 2015, 114, 2371-2379.	1.6	12
42	Mapping Vegetation-Covered Urban Surfaces Using Seeded Region Growing in Visible-NIR Air Photos. IEEE Journal of Selected Topics in Applied Earth Observations and Remote Sensing, 2015, 8, 2212-2221.	4.9	7
43	QoE-Oriented Two-Stage Resource Allocation in Femtocell Networks. , 2014, , .		21
44	ADDING ADAPTABLE TOE STIFFNESS AFFECTS ENERGETIC EFFICIENCY AND DYNAMIC BEHAVIORS OF LIMIT CYCLE WALKING. , 2014, , .		0
45	Molecular characterization and immune modulation properties of Clonorchis sinensis-derived RNASET2. Parasites and Vectors, 2013, 6, 360.	2.5	25
46	Validation of total ozone column derived from OMPS using ground-based spectroradiometer measurements. Remote Sensing Letters, 2013, 4, 937-945.	1.4	4
47	A Voxel-Based Method for Automated Identification and Morphological Parameters Estimation of Individual Street Trees from Mobile Laser Scanning Data. Remote Sensing, 2013, 5, 584-611.	4.0	189
48	The Carcinogenic Liver Fluke, Clonorchis sinensis: New Assembly, Reannotation and Analysis of the Genome and Characterization of Tissue Transcriptomes. PLoS ONE, 2013, 8, e54732.	2.5	77
49	Combined expression of antimicrobial genes (Bbchit1 and LJAMP2) in transgenic poplar enhances resistance to fungal pathogens. Tree Physiology, 2012, 32, 1313-1320.	3.1	41
50	Locating suitable roofs for utilization of solar energy in downtown area using airborne LiDAR data and object-based method: A case study of the Lujiazui region, Shanghai. , 2012, , .		6
51	Voxel-based Marked Neighborhood Searching method for identifying street trees using Vehicle-borne Laser Scanning data. , 2012, , .		4
52	Molecular Cloning and Characterization of Two Genes Encoding Dihydroflavonol-4-Reductase from Populus trichocarpa. PLoS ONE, 2012, 7, e30364.	2.5	41
53	Interactive expression design of multimedia maps based on flash. , 2011, , .		0